All-Atom Molecular Dynamics Simulations of the Temperature Response of Densely Grafted Polyelectrolyte Brushes

Harnoor Singh Sachar, Bhargav Sai Chava, Turash Haque Pial, and Siddhartha Das[a,*]

[a]Department of Mechanical Engineering, University of Maryland, College Park, MD 20742, United States

*sidd@umd.edu

Table of Contents Graphic

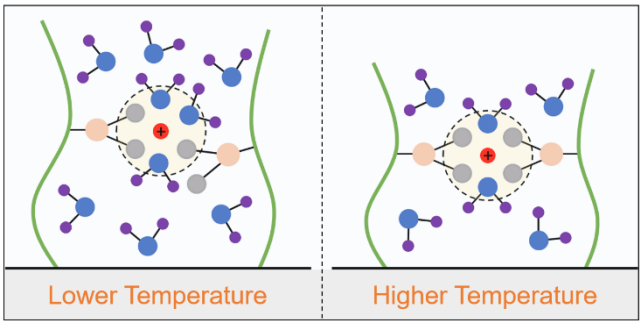

Abstract

Water acts a "good" solvent for most polyelectrolyte (PE) systems due to its high dielectric strength. Theoretical and experimental studies have highlighted some remarkably unconventional properties of strongly water-swollen PE brushes such as a reduction in brush height with increase in temperature. However, an understanding of the atomistic-scale response of the grafted PE chains as well as the local arrangement and organization of the brush-supported counterions and water molecules to changes in temperature is missing. Here, we conduct an all-atom molecular dynamics (MD) study to probe the influence of temperature on the "microstructure" of densely grafted, fully ionized polyacrylic acid (PAA) brushes. The atomistic insights obtained from our study shed light on prior experimental observations and elucidate the key role played by changes in hydrogen bonding network in dictating the hydrophilicity of the brushes. In addition to the temperature-mediated reduction in height of the PE brush layer, we study the influence of temperature on several properties of the brush-supported water molecules such as the number distribution and kinetics of water-water and water-PE hydrogen bonds (HBs), mass density, orientational tetrahedral order parameter, and the activation energy associated with the self-diffusion of water. The effect of temperature on the properties of the brush-trapped counterions is also quantified via changes in their solvation structure, counterion-water radial distribution function (RDF), and the translational mobility. Our findings unravel several hitherto unknown phenomena such as the enhanced propensity for attaining PE brush-induced "water-in-salt"-like scenarios at elevated temperatures, and an increase in the activation energy for the self-diffusion of water with increase in the degree of PE brush-induced nanoconfinement (from 'bulk water' to 'sparsely grafted PE brushes' to 'densely grafted PE brushes'). We anticipate that this work will be helpful in improving

our predictive capabilities of the temperature response of water-swollen PE brushes, which would be instrumental for better design of several PE brush systems used in a multitude of applications.

Introduction

Closely grafted polyelectrolyte (PE) chains are known to stretch out in the direction perpendicular to the grafting surface, and thereby form a "brush"-like configuration. Depending on the "regime" occupied by the grafted PE layer (as dictated by the brush grafting density, degree of polymerization, charge density of the chains, etc.), the swelling of the chains can result from a combination of various factors such as the electrostatic repulsion between the charged PE segments, the osmotic pressure of the brush-trapped counterions, and the excluded volume interactions.[1] By virtue of their unique topology, the brushes form an extremely interesting state of polymer/PE systems. Also, the large environmental-stimuli-responsiveness of the PE brushes have meant that they have found uses in a plethora of applications ranging from nanofluidic energy conversion,[2-3] current rectification,[4-5] and construction of nanomechanical gates,[6] to drug delivery,[7-8] oil recovery,[9] and colloidal stabilization.[10] Hence, it is not surprising that PE brushes have been studied extensively over the years by theoretical,[11-20] simulation-based,[21-30] as well as experimental studies.[31-40] However, an overwhelming majority of these studies have focused on the configurational changes associated with the PE chains, which we refer to as the brush "macrostructure", e.g., effect of external salt concentration on the height of the PE layer, monomer distribution profile, etc. There is a serious dearth of studies investigating the local arrangement, structure, and organization of the brush-trapped counterions and solvent molecules, or the "microstructure" of the grafted PE layers. e.g., role of ion-specific effects in dictating the hydrogen bonding network of the water molecules inside hydrophilic PE brushes. A comprehensive understanding of the "microstructure" is essential to several applications, since it is these small-scale features that ultimately dictate the bigger picture, i.e., the behavior of the brushes at much larger length scales. To fulfil the existing void in the literature, the Das group has utilized all-atom

molecular dynamics (MD) simulations to investigate the "microstructure" of water-swollen PE brushes with an unprecedented atomistic resolution.[41-43] Although some of these studies have provided extremely novel insights into the behavior of the PE brushes at an atomistic scale, such as the similarities between PE brushes and conventional "water-in-salt" systems,[41-42] several important questions remain unanswered. In the current manuscript, we investigate one such outstanding question - *How do changes in temperature influence the "microstructure" of strongly water-swollen PE brushes?* To be clear, we are interested in brushes that exhibit a gradual change in swelling with respect to temperature, instead of thermoresponsive brushes such as poly(*N*-isopropylacrylamide) (PNIPAM) that show an abrupt change in swelling behavior across a narrow temperature range. The choice of considering water as our solvent is a natural one, given that it is the most abundantly used "good" solvent for PE brushes, owing to its high dielectric constant.

Prior theoretical studies have revealed that hydrogen bonds (HBs) formed by the water molecules strongly influence the properties of hydrophilic polymer chains in solution as well as polymer brushes, especially their response to temperature.[44,45] However, these studies utilized a mean-field approach which did not yield any information about the temperature-mediated changes to the brushes at an atomistic level. While Dormidontova and coworkers went on to study the hydrogen bonding network in planar and spherical PEO brushes by employing all-atom MD simulations, they did not investigate the role of temperature on the properties of the HBs and consequently the properties of the PEO brushes.[46,47] A recent experimental study probed the effect of temperature on the hydrophilicity of several water-swollen polymer brushes [such as poly(*N*-isopropylacrylamide) (PNIPAM), poly(oligo[ethylene glycol] methyl ether methacrylate) (POEGMA), poly(2-[2-methoxyethoxy]ethyl methacrylate) ($PMEO_2MA$), poly(2-hydroxyethyl methacrylate) (PHEMA), and poly(2,5-dimethoxyaniline) (PDMA)] by utilizing techniques such

as ellipsometry and quartz crystal microbalance with dissipation monitoring (QCM-D).[48] Their ellipsometry and QCM-D measurements revealed an unconventional reduction in swelling coefficient with increase in temperature for strongly water-swollen POEGMA brushes. Moreover, their QCM-D measurements also indicated a decrease in the swelling coefficient of strongly water-swollen PDMA brushes with temperature (although this result was in contrast to their ellipsometry data). Even though they associated the observed changes in volume hydrophilicity to changes in solvent quality, their measurements were unable to provide a physical reasoning for such changes in solvent quality. Keeping all of this in mind, we conduct an all-atom MD simulation study to probe the effect of temperature on the configuration of strongly hydrophilic PE chains, and the local structure and arrangement of the brush-supported counterions and water molecules. It is important to understand that the high computational cost associated with all-atom MD simulations makes it impossible to study the experimentally accessible combinations of degree of polymerization and grafting density of the PE chains. Utilizing coarse graining approaches to investigate experimentally accessible parameter space, on the other hand, does not allow one to study the microstructure of the system, which is the main focus of the current manuscript. Thus, the trade-off between atomistic resolution and the ability of capture experimentally pertinent length scales is a necessary one, at least when it comes to molecular simulations.

In our simulations, fully ionized polyacrylic acid (PAA) chains (neutralized by Na^+ counterions) are chosen to represent the class of strongly water-swollen PE brushes due to their favorable interactions with water as a result of water-PAA hydrogen bonding (with water acting as the HB donor and the carboxylate oxygen of PAA acting as the HB acceptor). A snapshot of our MD simulation domain is depicted in Fig. 1.

Our results agree with the experimental observations indicating a reduction in height of strongly hydrophilic brushes with temperature.[48] We systematically explain how the reduction in water-water and water-PE HB strength is responsible for the lowering of solvent quality of the brushes with temperature, thereby reducing the extent of swelling of the PE chains along with an expulsion of water molecules from inside the grafted PE layer to the bulk. This expulsion of water molecules reduces the fraction of water-water and water-PE HBs inside the brushes. We also study the impact of temperature on various properties of the brush-trapped water molecules such as the mass density, orientational tetrahedral order parameter, and the translational mobility. Our analysis reveals a most interesting increase in the activation energy associated with the self-diffusion of water molecules with increase in the degree of brush-induced nanoconfinement (as one moves from 'bulk water' to 'sparsely grafted PE brushes' to 'densely grafted PE brushes'). In addition to the behavior of water molecules, we also analyze several properties associated with the brush-supported counterions. We reveal that the solvation structure of the counterions inside the PE brush layer changes significantly with temperature, as evident by an enhanced replacement of the solvation water with the electronegative atoms of the PE functional groups at elevated temperatures. Fascinatingly, despite the change in solvation structure of the counterions, the fraction of 'bound' water molecules (water present inside the first solvation shell of a counterion) remains invariant with temperature. In a prior study, we showed that PE brushes exhibit "water-in-salt"-like behavior ("water-in-salt" systems are highly concentrated aqueous electrolytes where the water supersedes the salt by both weight and volume[49,50]) at high grafting densities.[41] Our results indicate that such "water-in-salt"-like behavior can be triggered not only by increasing the PE brush grafting density but also by increasing the temperature for a given grafting density. We

conclude by investigating the role of temperature on the counterion-water radial distribution function (RDF) and the translational mobility of the brush-supported counterions.

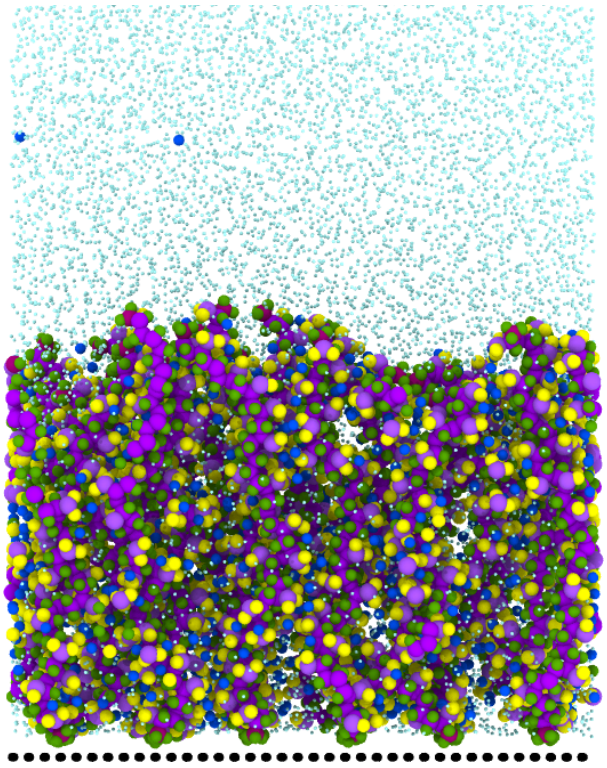

Figure 1: Snapshot of the MD simulation domain (truncated from the top) for grafting density, $\sigma_g = 0.1/\sigma^2$ and temperature, T=350 K. Atomic sizes are scaled proportional to their Lennard Jones (LJ) diameters. Dark blue spheres represent the Na^+ counterions, black spheres depict the discrete LJ wall, while the purple, green, and yellow spheres depict the carbon, hydrogen, and oxygen atoms of the fully ionized PAA chains, respectively. Water molecules are shown in reduced size to improve visualization.

Results and Discussions

Temperature driven decrease in the PE brush height

In this section, we discuss the effect of temperature on the equilibrium height of the PE brushes. Fig. 2 depicts the average end-to-end height ($< z_e >$) of the PE brush layer for various temperatures and grafting densities. $< z_e >$ is defined as the average vertical distance (in the direction perpendicular to the grafting surface) between the grafted and non-grafted terminal carbon atoms of the PAA chains. We observe that an increase in temperature leads to a reduction in brush height for both values of grafting densities. This temperature mediated decrease in brush height is consistent with previous experimental[48] and theoretical[45] studies on water swollen polymer brushes. Increasing the temperature leads to a reduction in hydrogen bonding between the neighboring water molecules (i.e., there is a reduction in the number of water-water HBs) as well as between the water molecules and PE functional groups (i.e., there is a reduction in the number of water-PE HBs). For our case, the oxygen atoms of the carboxylate functional group of the PAA chains or '$O_{Carbocylate}$' act as the HB acceptors and the hydrogen atoms of the water molecules or 'H_{Water}' act as the HB donors for the formation of the water-PE HBs. This reduction in the water-water and water-PE hydrogen bonding due to an increase in temperature is caused by the fact that the formation of the HBs is an enthalpically driven phenomenon. In other words, the formation of a HB is accompanied by a favorable change in enthalpy (i.e., $\Delta H < 0$) due to the favorable electrostatic interactions between the donor-acceptor pair participating in the HB. On the other hand, the HB formation also leads to an unfavorable change (i.e., a decrease) in the entropy of the participating species ($\Delta S < 0$) by limiting the number of available configurations required to ensure the existence of the HB: for example, an angle less than 30° between the (donor

Hydrogen)−(donor Oxygen)−(acceptor Oxygen) triads is required for the formation of water-water HBs.[50] Thus, the favorable change in enthalpy drives the formation of the HBs, while the unfavorable change of the entropy decreases the tendency to form the HB. This becomes evident by noting the free energy of HB formation, i.e., $\Delta G = \Delta H - T\Delta S$ (where T is the temperature). The above expression of ΔG also indicates that the free energy change associated with the HB formation becomes more unfavorable with an increase in temperature (given the fact that $\Delta S < 0$ for the HB formation). Such unfavourability in HB formation at an elevated temperature effectively implies a reduction in the water-water and water-PE HB strength within the grafted PE layer. Furthermore, the reduction in water-PE HB strength with temperature is much more pronounced in comparison to the reduction in water-water HB strength. This is evident from the fact that the fraction of water-PE HBs decays faster than the fraction of water-water HBs inside the brushes with an increase in temperature (see the subsection titled 'Hydrogen bonding' for more details). This behavior is consistent with prior studies on water swollen polyethylene oxide (PEO) brushes.[45] Given the competitive coexistence of the water-water and water-PE HBs, this results in a reduced relative favorability for the formation of water-PE HBs (as compared to the water-water HBs), which decreases the affinity for monomer-solvent contacts, thereby signaling a lowering of the solvent quality (the solvent quality is a measure of the favorability of monomer-solvent interactions over the monomer-monomer and solvent-solvent interactions). This reduction in solvent quality at elevated temperatures for water-swollen PAA brushes contrasts with the commonly observed increase in polymer swelling with temperature as predicted by the Flory-Huggins model.[51] The excluded volume (v) of a Kuhn segment of a PE chain in a solvent is a measure of the solvent quality and is given by:

$$v = a^3(1 - 2\chi), \qquad (1)$$

where a^3 is the volume of the Kuhn segment (a is the Kuhn length) and χ is the Flory-Huggins parameter. According to the Flory-Huggins theory,[51] χ depends on temperature as:

$$\chi = \frac{B}{T}, \qquad (2)$$

where B is a coefficient representing the enthalpic contribution to the energy of mixing between polymer and solvent. Thus, χ decreases with temperature leading to an increase in excluded volume interactions and thereby improving the solvent quality. Physically, this improvement in solvent quality results from the fundamental nature of the Lennard-Jones (LJ) interactions. As the temperature is increased, the LJ interactions between dissimilar species (in this case, the monomers-solvent interactions) become more favorable relative to those between similar species (in this case the monomer-monomer and solvent-solvent interactions). However, for the specific case of water-swollen brushes (such as PAA), this effect is dominated by changes to the HB network (as explained earlier) formed by the water molecules and PE functional groups. Thus, the solvent quality ends up decreasing with the temperature and the mixture (PE + water) shows a LCST (lower critical solution temperature) behavior. The classical form of the Flory-Huggins model (see eq. 2) is unable to capture this LCST behavior. A way around this issue is to consider an effective Flory Huggins parameter, $\chi_{eff}(T, \phi)$ that depends on both temperature as well as the polymer/PE volume fraction ϕ [instead of the usual $\chi(T)$]. This approach allows for the inclusion of entropic contributions such as the variation in free energy of HB formation with temperature and polymer/PE volume fraction for water-swollen polymer brushes. Several studies have derived and/or fitted the mathematical form of $\chi_{eff}(T, \phi)$ for different polymer-solvent mixtures and obtained an excellent match with the experimentally observed phase diagram of these systems.[52-53]

A "poorer" solvent quality implies that the excluded volume effect of the brushes, which can support the elastic energy of the brushes (which has an entropic origin), is significantly lowered. This ensures a much smaller extension of the brushes (a larger extension would have meant a larger elastic energy change): therefore, with an increase in temperature, there is a decrease in the brush height and a consequent expulsion of water molecules from inside the grafted PE layer to the bulk. Now, it is important to note that the swelling of PE brushes is dictated by a combination of factors such as intersegmental electrostatic repulsion, osmotic pressure of the brush-trapped counterions, and the excluded volume interactions (the relative contribution of these factors depends on properties of the grafted chains such as the degree of polymerization, grafting density, etc.). On the contrary, the swelling of polymer (neutral) brushes is solely a consequence of the excluded volume interactions. As a result, a reduction in solvent quality (and thereby a lowering of the excluded volume interactions) with temperature leads to a much more prominent reduction in height of polymer brushes in comparison to PE brushes. In other words, the repulsive electrostatic interactions due to the charges present on the grafted chains mitigate the reduction in brush height with temperature for water-swollen PE brushes. Moreover, the electrostatic interactions also cause an additional stiffening of the PE chains (as quantified by an increase in their persistence length), which decreases their flexibility and results in an enhanced resistance to change in brush height. Note that a recent theoretical study on simultaneous temperature and pH responsive polymer brushes by Morochnik *et al*[54] predicts that the temperature-mediated decrease in brush height is weaker at higher values of pH [see Fig. 4(a) and S4 in Ref. 54], which corresponds to fully ionized PE chains such as the ones considered in our study. The stiffness of tethered PE chains also increases with the grafting density, which explains the relatively smaller decrease in brush height with temperature for higher grafting density of the brushes ($\sigma_g = 0.2/\sigma^2$) in Fig. 2.

The reason for the modest reduction in brush height (see Fig. 2) observed in our simulations can be attributed to a combination of low degree of polymerization and high grafting density of the PE chains, both of which lead to a significant enhancement in the persistence length (and thereby a reduced flexibility) of the grafted chains. However, we must point out that the impact of this study lies in the qualitative (rather than quantitative) changes of the brush properties with temperature that are reported. A greater change in brush height with temperature will be anticipated for relatively longer and sparser brushes (where the brush height is several times greater than the persistence length) which are abundantly used in experimental studies, assuming that the mechanism for variation in brush height remains the same.

In order to intuitively understand the correlation between the reduction in brush height and the expulsion of water molecules from inside the grafted PE layer, we assume a uniform monomer distribution inside the PE brushes (the Alexander-de-Gennes model[55-56]). In fact, several studies have shown that this is a reasonable assumption for densely grafted PE brushes.[21] Under this condition, the brush height can be expressed as[57-58]:

$$H = \frac{\sigma_g N a^3}{\phi}, \qquad (3)$$

where H is the equilibrium brush height, σ_g is the PE brush grafting density, N is the number of Kuhn monomers per chain, and ϕ is the PE volume fraction. Notice that ϕ is assumed to be a constant throughout the brush height, in line with the Alexander-de-Gennes model. Mathematically, ϕ can be written as:

$$\phi = \frac{N a^3}{N a^3 + \frac{n_w v_w}{\sigma_g}}, \qquad (4)$$

where n_w represents the number of water molecules per unit area inside the PE brush layer, and v_w is the net volume occupied by each water molecule. Assuming that the packing efficiency of the PE-solvent system remains invariant of ϕ, we can treat v_w as a constant. From equations 3 and 4, we can infer that a decrease in brush height leads to an increase in ϕ, and thereby a decrease in the number of water molecules per unit area within the PE brush layer (n_w). This explains the aforementioned expulsion of water molecules from the PE layer into the bulk with an increase in temperature.

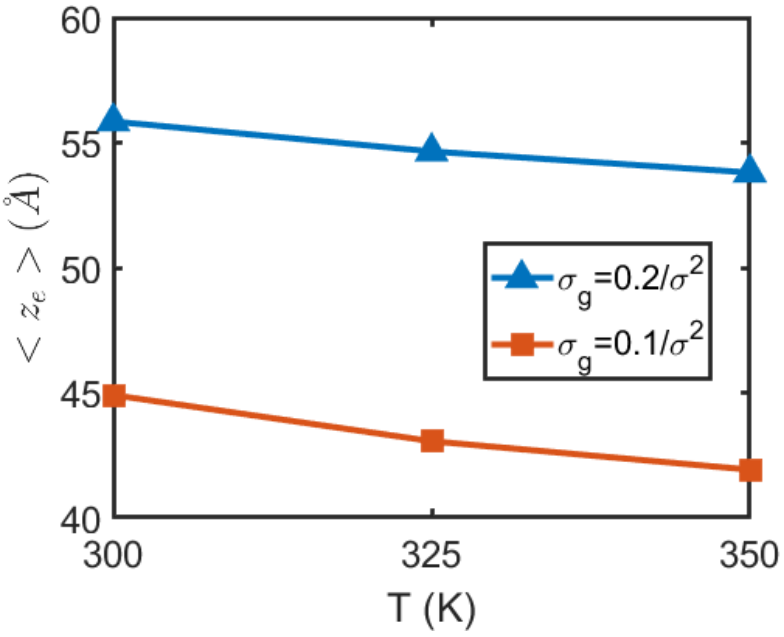

Figure 2: Variation in the average end-point brush height with temperature for different PE brush grafting densities

Effect of temperature on the properties of PE brush-trapped water molecules

Hydrogen bonding

In the last section, we discussed the temperature-mediated reduction in the PE brush height and the corresponding expulsion of water molecules from the grafted PE layer. Now, we shift our attention to the effect of temperature on the water-water and water-PE HB characteristics inside the brushes as quantified by their average numbers and lifetime. We define a HB to exist if the following conditions are satisfied: the distance between the donor-acceptor pair, r<3.5 Å and the angle formed by the (donor Hydrogen)−(donor Oxygen)−(acceptor Oxygen) triad, θ<30°.[50] We quantify the changes in hydrogen bonding network by investigating the fraction of water-water and water-PE HBs inside the brushes. The fraction of water-water (water-PE) HBs associated with a water molecule ($O_{Carboxylate}$ atom) is defined as the ratio of the number of water-water (water-PE) HBs formed by that water molecule ($O_{Carboxylate}$ atom) to the maximum number of water-water (water-PE) HBs that can be formed by a water molecule ($O_{Carboxylate}$ atom). We consider a maximum of 4 water-water HBs per water molecule and 2 water-PE HBs per $O_{Carboxylate}$ atom for the calculation of HB fraction, which is similar to Ref. 45 for water-swollen PEO brushes. The average fraction of water-water HBs ($\bar{n}_{HB,wat-wat}$) inside the PE brushes decreases with an increase in temperature [see Fig. 3; see Fig. S2 in the Supporting Information (SI) for the transverse distribution of the fraction of water-water HBs]. In addition, the average fraction of water-PE HBs ($\bar{n}_{HB,wat-PE}$) inside the grafted PE layer also diminishes at elevated temperatures (see Fig. 3). The reason for both these trends is two-fold. First, an increase in temperature decreases the free energy associated with water-water and water-PE HB formation (please see the discussion in the previous subsection). This reduction in the free energy of HB formation reduces the thermodynamic propensity for the formation of water-water and water-PE HBs. Second, a reduction in the height

of the PE brush layer with rise in temperature increases the PE volume fraction (ϕ) inside the brushes (see eq. 3). Prior studies by Szliefer *et al*[45] (for PEO brushes) and Dahal *et al*[46-47] (for PEO in solution) have shown that an increase in the polymer volume fraction is directly correlated to a decrease in the fraction of water-water and water-polymer HBs. This decrease in the fraction of HBs is associated with a depletion in the number of HB donors/acceptors (donors) available for the formation of the water-water (water-PE) HBs.[45] Please note that the decrease in fraction of water-water and water-PE HBs with an increase in temperature and grafting density are consistent with the theoretical predictions of Ref. 45 for water-swollen PEO brushes. In addition, similar to Ref. 45, we observe that the fraction of water-PE HBs decays much faster than the fraction of water-water HBs inside the brushes with an increase in temperature (with an increase in temperature from 300 K to 350 K, the fraction of water-water HBs decreases by ~0.036 and ~0.045 for $\sigma_g = 0.1/\sigma^2$ and $\sigma_g = 0.2/\sigma^2$ respectively, while the fraction of water-PE HBs decreases by ~0.129 and ~0.107 for $\sigma_g = 0.1/\sigma^2$ and $\sigma_g = 0.2/\sigma^2$ respectively). This indicates that the strength of water-PE HBs decreases much faster than the water-water HBs with an increase in temperature (i.e., the formation of water-PE HBs becomes unfavorable relative to water-water HBs), which justifies the decrease in solvent quality and the corresponding reduction in brush height observed in Fig. 2.

Szliefer *et al*[45] reports a decrease of ~0.07 for the fraction of water-water HBs, and a decrease of ~0.13 for the fraction of water-PEO HBs, as the temperature is increased from 10℃ to 80℃ (see Fig. 2 in Ref. 45). Thus, a quantitative comparison reveals that the scale of variation in the fraction of water-water and water-PE HBs observed in our simulations is comparable to the theoretical predictions made by Szliefer *et al*[45] for water-swollen PEO brushes. This shows that the changes

in fraction of HBs observed in our system are significant and in line with the predictions of prior studies.

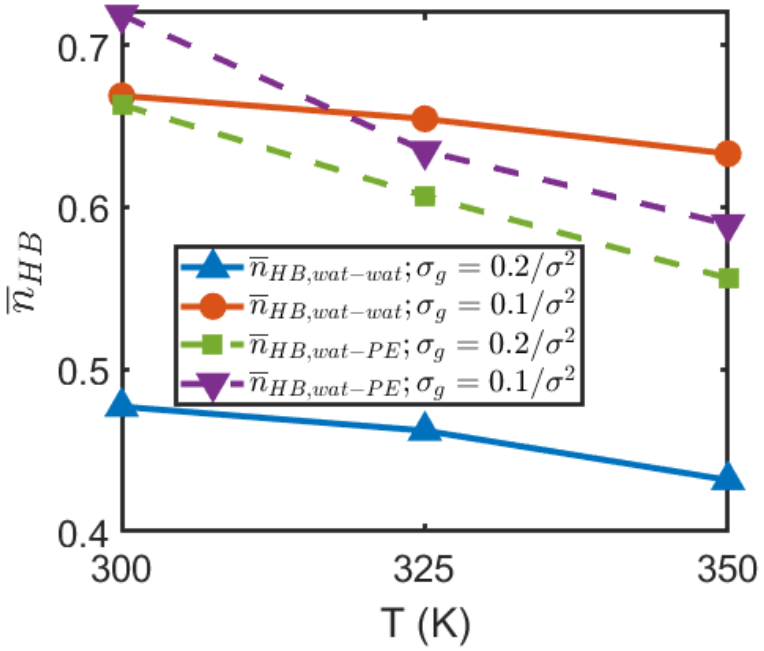

Figure 3: Variation of the average fraction of water-water HBs ($\bar{n}_{HB,wat-wat}$) and the average fraction of water-PE HBs ($\bar{n}_{HB,wat-PE}$) with temperature inside the PE brushes for different grafting densities.

Next, we investigate the stability of the water-water and water-PE HBs from a kinetics point of view. To quantify the HB kinetics, we plot the residence time (R_{HB}) distribution for water-water [see Fig. 4(a) and Fig. S6(a)] and water-PE HBs [see Fig. 4(b) and Fig. S6(b)] at different temperatures. $R_{HB}(t)$ denotes the average fraction of HBs that exist at time t (without breaking in the time interval [0,t]), given that they were formed at t=0.[50] R_{HB} provides a measure of the short time scale stability of the HBs and is an excellent tool to study the effect of thermal fluctuations on the fast HB kinetics. First, we see that the R_{HB} corresponding to water-water HBs decays much more quickly inside the brushes as compared to bulk (at the same temperature) indicating that the water-water HBs are less stable (at short time scales) within the PE brush layer. In fact, the decay of R_{HB} is much faster at higher grafting density of the PE chains ($\sigma_g = 0.2/\sigma^2$). A prior study on "water-in-salt" solutions by Han *et al* reported that the relaxation time for fast dynamics of water-water HBs decreased with an increase in salt concentration.[50] The PE brush-counterion-water system studied in our manuscript also exhibits a "water-in-salt"-like behavior (see the subsection titled 'Counterion solvation structure'). An increase in grafting density of the PE chains corresponds to an increase in the counterion concentration within the brushes, which is analogous to an increase in 'salt concentration' of conventional "water-in-salt" systems. Thus, the decrease in R_{HB} of water-water HBs from bulk water to sparsely grafted brushes to densely grafted brushes observed in our study is consistent with the results of Han *et al*.[50] Han attributed the faster decay of HBs to enhanced thermal fluctuations in the system at high salt concentration. We believe that the same reasoning applies to our system, where in the thermal fluctuations increase with an increase in the grafting density of the PE chains. Secondly, we observe that the R_{HB} decays faster at elevated temperatures, for both water-water and water-PE HBs, resulting in a reduced average HB lifetime (area under the R_{HB} vs t curve). Thus, we have established that the water-water and

water-PE HBs inside the brushes not only become scarcer but also become kinetically unstable at elevated temperatures.

Finally, we observe that R_{HB} decays much faster for the water-water HBs as compared to water-PE HBs, thereby resulting in a higher average lifetime for the water-PE HBs (in comparison to water-water HBs). The reason for this finding was discussed in our prior manuscript,[43] albeit for the HB correlation function C_{HB} (which captures slow HB dynamics) instead of the residence time distribution R_{HB} (which captures fast HB dynamics) discussed in the current manuscript. However, the reasoning remains the same and we reiterate it here for improved readability. Hydrogen bonding reduces the entropy ($\Delta S < 0$) of the participating species by restricting the number of conformations available to the donor and acceptor molecules relative to each other. E.g., a commonly used criteria for the formation of water-water HBs requires that the distance between the acceptor oxygen and donor oxygen is less than 3.5 Å, and the angle formed by the (acceptor oxygen) – (donor oxygen) – (hydrogen) triad is less than 30°.[50] As a result, water molecules lose a significant amount of entropy upon HB formation. On the other hand, PE functional groups are connected to the backbone of the grafted PEs. The presence of these topological constraints ensures that the PE functional groups do not lose much entropy upon the formation of water-PE HBs. Therefore, there is a higher entropy loss associated with the water-water HBs in comparison to water-PE HBs. This destabilizes the water-water HBs from both thermodynamics (as quantified by a decrease in the magnitude of Gibbs free energy of HB formation, $\Delta G = \Delta H - T\Delta S$) and kinetics (as quantified by a smaller average lifetime of the HBs) standpoint. This explains the faster decay of R_{HB} associated with water-water HBs.

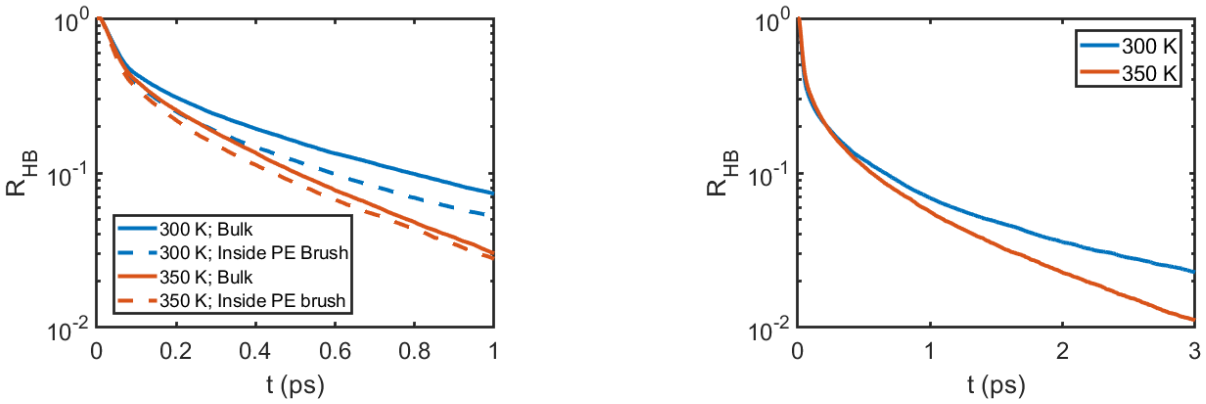

(a) **(b)**

Figure 4: (a) Residence time distribution for water-water HBs as a function of temperature in bulk water and inside PE brushes with $\sigma_g = 0.1/\sigma^2$. (b) Residence time distribution for water-PE HBs as a function of temperature inside PE brushes with $\sigma_g = 0.1/\sigma^2$.

Mass density

The increase in polymer volume fraction (ϕ) triggered by an expulsion of water molecules at higher temperatures results in a decrease in the mass density of water (ρ_w) within the PE brushes. Fig. 5 depicts the transverse mass density distribution of water within the grafted PE layer as a function of temperature. We can observe that the decrease in mass density of the water with an increase in temperature becomes much more significant at higher degrees of PE brush-induced confinement, i.e., as one moves from bulk water to sparsely grafted PE brushes to densely grafted PE brushes.

Interestingly, from Fig. 5, we can observe that the density of water passes through a minimum near the PE brush - bulk water (or simply the brush-water) interface. This is due to an accumulation of counterions inside the electric double layer (EDL) present above the non-grafted end of the chains, which significantly increases the counterion concentration near the brush-water interface. This can be confirmed by the presence of a net positive charge near the brush-water interface for fully ionized PAA brushes neutralized by Na^+ counterions in Fig. S3 of Ref. 41. As a result, there is a partial exclusion of water molecules near the tip of the brushes due to steric effects imposed by the presence of a large concentration of counterions. This explains the observed non-monotonic variation of the mass density of water (as a function of distance from the grafting surface) as well as the minima of water density at the brush-water interface.

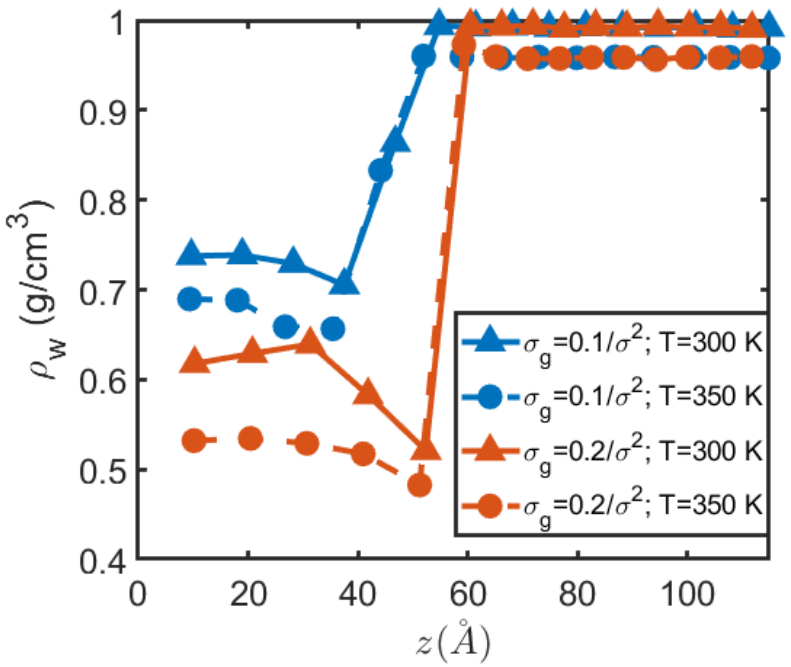

Figure 5: Transverse distribution of the mass density of water for various combinations of temperatures and PE brush grafting densities.

Orientational tetrahedral order parameter

The orientational tetrahedral order parameter (q) provides a measure of the local arrangement of water molecules in a system.[59] Larger values of q indicate a more 'tetrahedron'-like arrangement of the neighboring water molecules, while smaller values of q indicate progressively higher deviations from a tetrahedral arrangement. Mathematically, q=1 corresponds to a perfectly tetrahedral arrangement of water and q=0 corresponds to the case of an ideal gas. From Fig. 6, we can observe that the probability distribution of q in bulk water (for both T=300 K and T=350 K) consists of a combination of a peak and a shoulder. This peak and shoulder for bulk water arise from distinct populations of water molecules corresponding to local tetrahedral and non-tetrahedral environments.[60,61] Furthermore, the probability distribution of q shifts towards lower values with an increase in temperature, both for bulk water and water trapped inside the PE brushes (see Fig. 6). This is attributed to a decrease in the average fraction of water-water HBs at elevated temperatures (see Fig. 3). However, the shift in q is less prominent for water molecules inside the PE brushes as compared to bulk water. This can be explained by looking into the probability distribution of the number of water-water HBs formed by the water molecules at different temperatures and degrees of brush-induced confinement (see Fig. S3). A tetrahedral arrangement of water molecules is achieved in liquid water when the water molecules form 4 water-water HBs with their neighbors (2 as HB donors and 2 as HB acceptors). Thus, a change in the percentage of water molecules participating in identically 4 water-water HBs should significantly impact the probability distribution of q. From Fig. S3, we can see that the percentage of water molecules forming 4 water-water HBs in bulk water drops from 52.39% at 300 K to 40.38% at 350 K (a decrease of 12.01%). In comparison, the fraction of water molecules forming 4 water-water HBs changed form 22.49% at 300 K to 18.77% at 350 K (a decrease of only 3.72%) inside the PE

brushes with $\sigma_g = 0.1/\sigma^2$ (the percentage change is even lesser for $\sigma_g = 0.2/\sigma^2$). This makes intuitive sense since the fraction of water molecules forming 4 water-water HBs inside the grafted PE layer is very small even at lower temperatures. Therefore, an increase in temperature is unable to drastically alter the percentage of such water molecules (forming 4 water-water HBs). Hence, we have established that the decrease in fraction of water molecules forming 4 water-water HBs with temperature is much more significant in bulk water than that inside the PE brush layer. This explains the relatively smaller temperature-mediated shift in the probability distribution of q within the PE brushes as compared to bulk water.

Hydrophilic PE brushes are typically associated with the formation of water-PE HBs. These water-PE HBs are in competitive coexistence with the water-water HBs and thereby reduce the fraction of water-water HBs inside the brushes as compared to bulk water. A quick glance at Fig. S3 confirms a significant decrease in the percentage of water molecules forming 4 water-water HBs inside the brushes in comparison to bulk. As a result, the local arrangement of water molecules inside the brushes shows a higher deviation from tetrahedral arrangement. Since, most hydrophilic PE brushes contain functional groups that can form HBs with the water molecules, we anticipate a decrease in the tetrahedral arrangement of water molecules inside hydrophilic PE brushes in general (and not just for water swollen PAA brushes). A prior computational study by Lee *et al* revealed that the local tetrahedral structure of water is distorted in the vicinity of carbohydrate molecules such as trehalose, glucose, and sucrose, all of which can form HBs with the water molecules.[62]

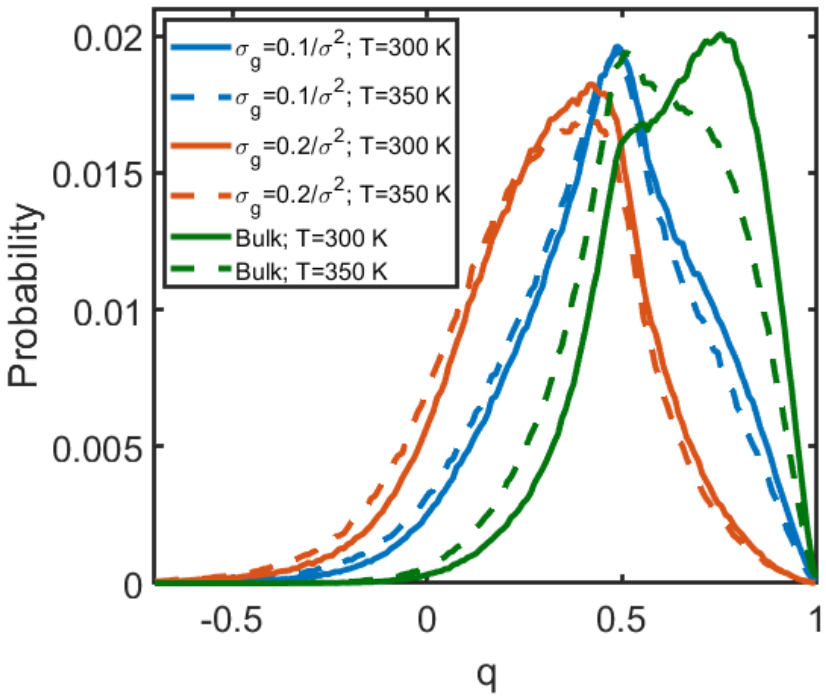

Figure 6: Probability distribution of the orientational tetrahedral order parameter (q) as a function of temperature under different degrees of PE brush-induced nanoconfinement.

Translational mobility of water

We observe an increase in the mobility of water molecules inside the brushes (as quantified by their mean squared displacement or MSD) with an increase in temperature (see Fig. S4 in the SI). The PE brush-trapped water molecules can be classified into two categories, namely 'bound' and 'free' water molecules.[42] 'Bound' water molecules are those that are present inside the first solvation shell (r < 3.2 Å) of at least one Na^+ counterion. Any water molecule that does not satisfy this criterion is referred as a 'free' water molecule. 'Free' water molecules are the major contributors to the overall mobility of the brush-trapped water due to a strong association of the 'bound' water molecules to the relatively immobile counterions (see the discussion in subsection titled 'Translational mobility of counterions'). Our simulations indicate that the percentage of 'bound' water molecules remains invariant with temperature (approx. 36% for $\sigma_g = 0.1/\sigma^2$ and approx. 64% for $\sigma_g = 0.2/\sigma^2$; see Fig. S5 in the SI), the reasons for which will be discussed in the subsection titled 'Counterion solvation structure'. Therefore, an increase in the water mobility translates to an increase in the mobility of 'free' water molecules within the grafted PE layer.

Next, we study the self-diffusion coefficient (D_w) associated with the water molecules at different temperatures and different degrees of brush-induced confinement. The self-diffusion coefficients were obtained by applying a linear fit to the latter half (25-50 ps) of the MSD vs time curves (see Fig. S4 for the MSD vs time curves for water molecules) to avoid any influence of the initial ballistic regime.[63] Fig. 7(a) plots the self-diffusion coefficients for various cases as a function of the inverse temperature. We observe that the self-diffusion coefficients follow the Arrhenius equation even inside the PE brushes, as evident from the linear relationship between D_w and 1/T in the log-log scale. Thus, we have established that the Arrhenius equation can be used to model the effect of temperature on the self-diffusion coefficient of water molecules inside densely grafted

PE brushes. In order to obtain the activation energy (E_a) associated with different degrees of PE brush-induced nanoconfinement, we fitted the self-diffusion coefficients vs inverse temperature curves to the Arrhenius equation, as given below:

$$D_w = D_{0,w} \exp\left(-\frac{E_a}{k_B T}\right), \qquad (5)$$

where $D_{0,w}$ is a pre-factor whose value depends on the frequency of diffusion attempts and k_B is the Boltzmann constant. Fig. 7(b) depicts the value of E_a as a function of the PE brush grafting density. We obtain an activation energy of 3.12 kcal/mol for bulk water at 300K, which is in excellent agreement with the value of 3.1 kcal/mol (over the temperature range 300K – 500K) reported by a prior MD study on SPC/E water.[64] Furthermore, we observe a progressive increase in the activation barrier with an increase in the degree of PE brush-induced confinement (from 'bulk water' to 'sparsely grafted PE brushes' to 'densely grafted PE brushes'). This increase in the activation energy can be attributed to an increase in the number density of charge bearing species inside the grafted PE layer at higher grafting densities, which leads to an enhancement in the magnitude of the local electric fields present inside the brushes. As a result, the potential energy curve becomes much steeper and the water molecules need to overcome a higher activation barrier to migrate from one site to another.

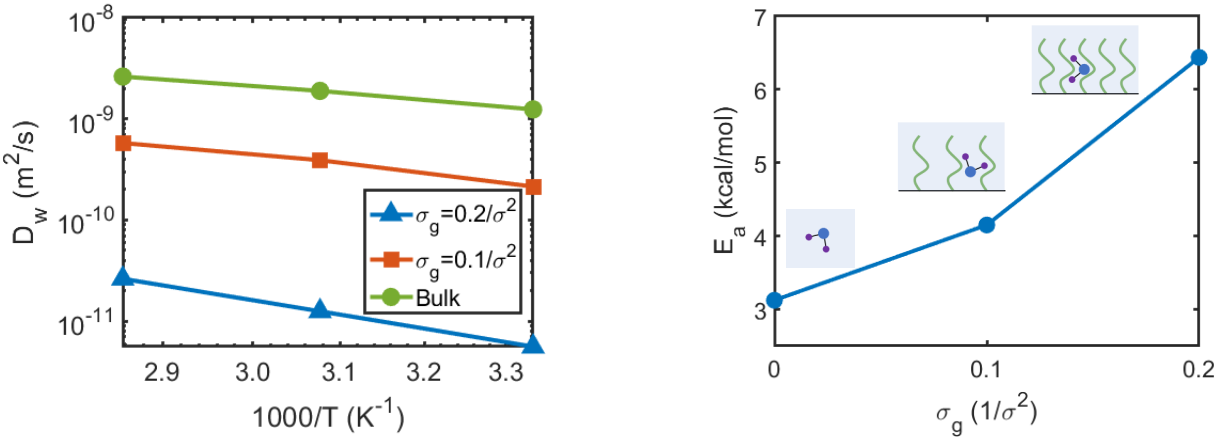

(a) **(b)**

Figure 7: (a) Self-diffusion coefficient for water as a function of the inverse temperature (plotted in log-log scale) for different degrees of brush-induced confinement. (b) Activation energy for the self-diffusion of water under various degrees of brush-induced nanoconfinement (these different degrees of brush-induced confinements have been depicted in the insets of the figure). $\sigma_g = 0$ represents the case of bulk water.

Effect of temperature on the properties of PE brush-trapped counterions

Counterion solvation structure

In this section, we shift our attention to the influence of temperature on the local structure, arrangement, and distribution of the PE brush-trapped counterions. Our choice of grafting densities is high enough to ensure that the brushes are present in the osmotic brush regime.[41] One of the characteristics of this regime is that most of the counterions are trapped inside the PE brush layer. This is observed to be the case in our MD simulations as well, where all the counterions are observed to be present within the grafted PE layer for all the probed values of temperatures and grafting densities. We have already established that an increase in temperature leads to a reduction in the brush height (see Fig. 2). Moreover, the mass density of water inside the brushes itself decreases with temperature (see Fig. 5). These results, coupled with the fact that the counterions do not escape the PE brush layer, lead to an increase in the counterion molarity/molality within the PE brush layer at elevated temperatures.

As established in our prior publications,[41-42] there is a replacement of the solvation water of the Na^+ counterions by the oxygen atoms of the carboxylate functional groups ($O_{Carboxylate}$) of the PAA chains inside the brushes. The replacement of solvation water occurs in a way that preserves the overall solvation number of the Na^+ counterions. We observe that this replacement of solvation water is enhanced at elevated temperatures [see Fig. 8(a) and Fig. S7(a)]. This is attributed to the entropic cost associated with the 'bound' water molecules. From an entropic standpoint, it is favorable for the $O_{Carboxylate}$ atoms to "solvate" the counterions as compared to water molecules. This is because the $O_{Carboxylate}$ atoms are tethered to the PE chains, and are thereby unable to drift freely due to chain connectivity. As a result, there is very little loss of entropy associated with an $O_{Carboxylate}$ atom solvating a counterion. On the other hand, water molecules are mobile species and

lose significant entropy when bound to a counterion. Accordingly, with an increase in temperature, as the entropic effects start to dominate over their enthalpic counterparts, there occurs an enhanced replacement of solvation water of the counterions by the $O_{Carboxylate}$ atoms. The average number of solvation water molecules associated with the brush-supported counterions changes from 2.95 at 300 K to 2.48 at 350 K for $\sigma_g = 0.2/\sigma^2$ [see Fig. S7(a)]. This corresponds to a change of approximately 0.47 solvation water molecules per counterion (the number remains similar for $\sigma_g = 0.1/\sigma^2$). The release of a single solvation water molecule can lower the free energy of the system by ~1k_BT. This translates to a reduction in the free energy of the PE brush-counterion-water system by ~0.5 k_BT per unit brush-trapped counterion in our simulations. Thus, the variation in solvation structure of the counterions with temperature observed in our simulations is extremely consequential in dictating the behavior of the brushes. In addition, we observe that the replacement always occurs in a way that maintains a near constant solvation number (~6) with respect to temperature.

It is important to note that an enhanced replacement of the solvation water of the brush-trapped counterions with temperature means that a greater number of counterions are surrounding (and thereby screening) the $O_{Carboxylate}$ atoms, which would lead to better local neutralization of the charged PE functional groups. This will reduce the intersegmental repulsion between the PE chains and contribute to the reduction of brush height observed in Figure 2. Unlike the relative variation of water-water and water-PE HBs, this mechanism for brush height reduction with temperature is unique to charge-bearing PE brushes (and not found in neutral polymer brushes like PEO).

In the subsection titled ‘Translational mobility of water’, we had mentioned that the percentages of ‘free’ and ‘bound’ water molecules within the PE brushes remains unchanged with an increase in temperature. Here, we explain why this is the case. On the one hand, an increase in temperature

forces some of the 'free' water molecules to be expelled outside the grafted PE layer due to a reduction in brush height (see the discussion in subsection titled 'Temperature driven decrease in the PE brush height'). This tends to decrease the percentage of 'free' water molecules inside the grafted PE layer. On the other hand, increase in temperature leads to an enhanced replacement of the solvation water of the Na^+ counterions by $O_{Carboxylate}$ atoms [see Fig. 8(a) and Fig. S7(a)]. Thus, some of the 'bound' water molecules get converted to 'free' water molecules. This tends to increase the percentage of the 'free' water molecules. Fascinatingly, the two phenomena nullify each other and ensure that the percentage of 'free' water molecules remains constant with respect to temperature (for a specific grafting density). A schematic representation of the changes in PE brush height, variation of the counterion solvation structure, and the invariance of the percentage of 'bound' water molecules (inside the PE brushes) with temperature is provided in Fig. 8(c).

Next, we study the influence of temperature on the PE brush-induced "water-in-salt"-like scenarios. "Water-in-salt" systems are super concentrated aqueous electrolytes where the salt overwhelms the water in terms of both mass and volume.[49,50] In other words, "water-in-salt" solutions contain a mixture of water molecules and salt (ion-pairs) in a proportion such that the salt is the dominant species by both weight and volume (as opposed to usual salt solutions where the water molecules are the dominant species). Conventional "water-in-salt" systems contain salts that comprise of a small cation and a bulky anion. E.g., Lithium bis(Trifluoromethanesulfonyl)imide or LiTFSI. Our previous publications revealed that densely grafted PE brushes show a "water-in-salt"-like behavior with the PE-repeating-unit−counterion complex playing the role of the 'salt'.[41-42] The PE repeating units [$-CH_2-CH(COO^-)-$ in our case] act as the anions and the counterions (Na^+ in our case) act as the cations of this 'salt'. Fig. 8(b) plots the 'salt' [$RCOO^-Na^+$; R: CH_2-CH] to water ratio (by mass and volume) inside the brushes

for $\sigma_g = 0.1/\sigma^2$ [plot for $\sigma_g = 0.2/\sigma^2$ is provided in Fig. S7(b) of the SI] as a function of temperature (bottom axis) and counterion molality (top axis). We observe a monotonic increase in the 'salt' to water mass and volume ratios with an increase in temperature. This is the result of an enhanced counterion concentration (and thereby an enhanced 'salt' concentration) inside the grafted PE layer at elevated temperatures. Furthermore, we see that the 'salt' surpasses the water by both mass and volume (inside the PE brush layer) at some temperature between 325 K and 350 K (for $\sigma_g = 0.1/\sigma^2$). In other words, the PE brush-counterion-water system exhibits a "water-in-salt"-like behavior above a critical temperature (which lies between 325 K and 350 K for $\sigma_g = 0.1/\sigma^2$). Therefore, we have established that PE brush-induced "water-in-salt"-like behavior can be obtained not only by increasing the grafting density of the brushes (as elucidated in Ref. 41) but also by increasing the temperature of the PE brush-counterion-water system.

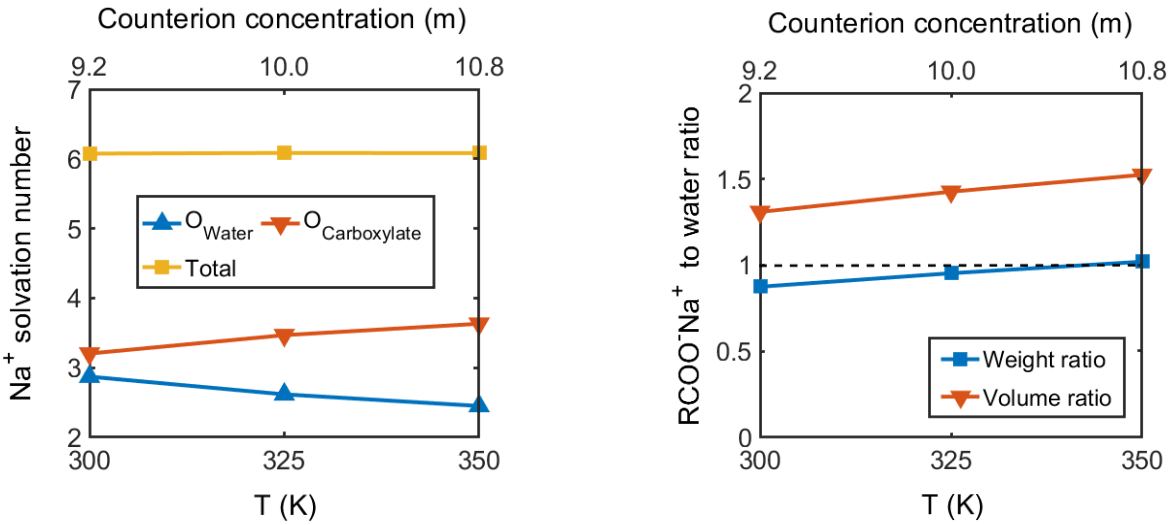

(a)

(b)

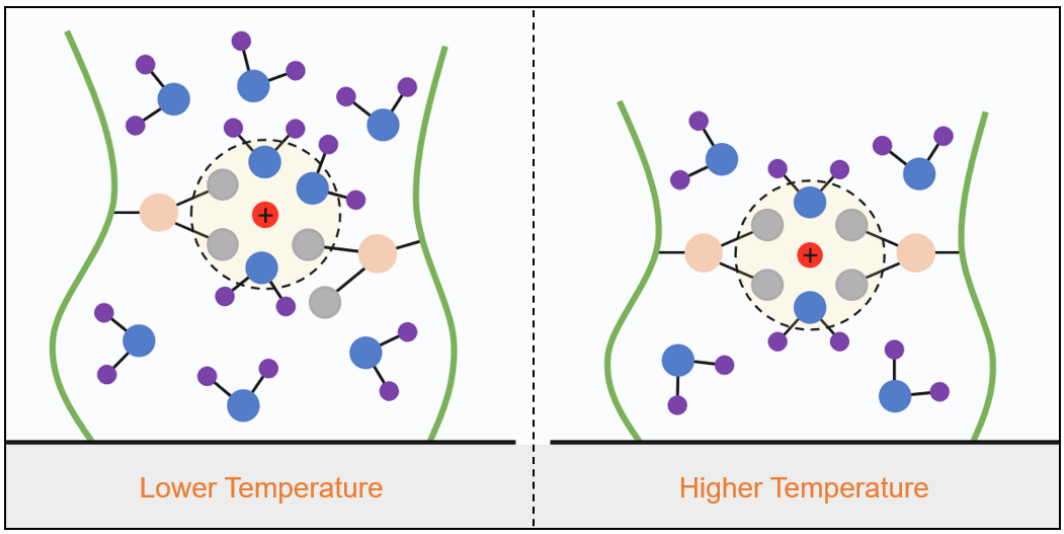

(c)

Figure 8: (a) Variation of the counterion solvation structure inside the grafted PE layer ($\sigma_g = 0.1/\sigma^2$) with temperature (bottom axis) and counterion molality (top axis). (b) Variation of the 'salt' to water ratio by mass and volume inside the PE brush layer ($\sigma_g = 0.1/\sigma^2$) with temperature (bottom axis) and counterion molality (top axis). (c) Schematic depicting the effect of temperature

on the counterion solvation structure in addition to the invariance of the percentage of 'bound' water molecules (with temperature) inside the PE brushes. Notice the decrease in height of the grafted PE layer at higher temperature. The backbones of the grafted PE chains are depicted as green curves, the Na^+ counterions are depicted as red circles, while the carboxylate oxygen, carboxylate carbon, oxygen of water, and hydrogen of water are depicted in grey, beige, blue, and purple circles, respectively. The yellow circle with a dashed outline represents the first solvation shell of the Na^+ counterions.

Counterion-water radial distribution function (RDF)

Fig. 9 plots the Na^+-O_w (O_w represents the oxygen atoms of water molecules) radial distribution function (RDF) in "bulk" (0.1 molal aqueous solution of NaCl) as well as inside the PE brushes with $\sigma_g = 0.1/\sigma^2$. Qualitatively similar results were found for $\sigma_g = 0.2/\sigma^2$ (see Fig. S8 in the SI). For the calculation of Na^+-O_w RDF, we have considered counterions and water molecules buried deep within the brushes (far away from the brush-water interface and the grafting surface). Inside the brushes, the height of the first peak of the Na^+-O_w RDF decreases as compared to in the "bulk". This is because of the tremendous replacement of solvation water of the counterions by the $O_{Carboxylate}$ atoms. With an increase in temperature (for a given grafting density), the replacement of solvation water of the counterions is more pronounced [see Fig 8(a) and Fig. S7(a)] within the PE brushes. This tends to decrease the height of the first peak of the Na^+-O_w RDF. However, the mass density of water molecules within the brushes decreases with an increase in temperature (see Fig. 5). This will tend to increase the height of the first Na^+-O_w RDF peak as the RDF is normalized with the respect to the overall water density within the brushes. The decrease in solvation water dominates over the effect associated with the reduction in mass density of water, and therefore, we observe a lowering of the first peak of the Na^+-O_w RDF within the PE brush layer with increasing temperature.

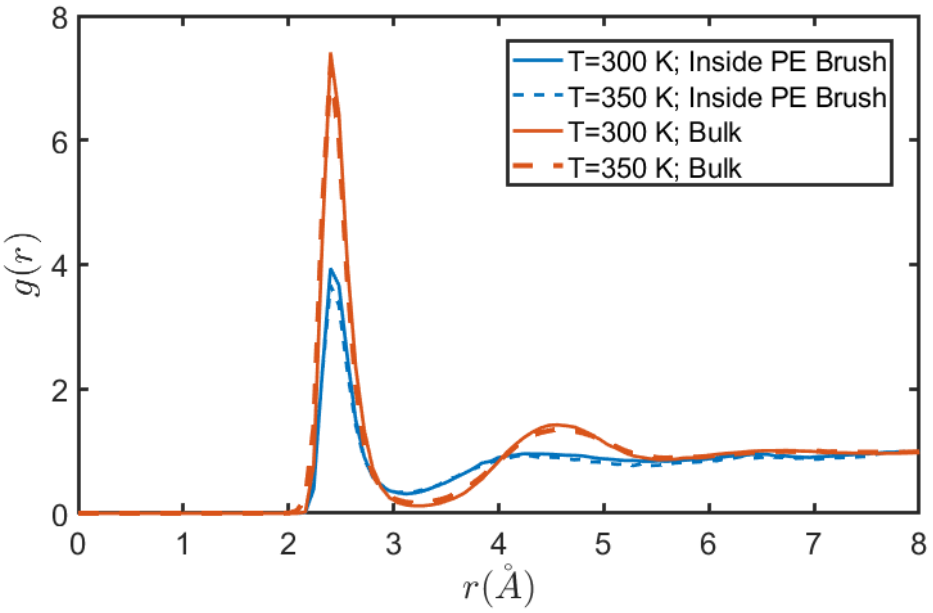

Figure 9: Na^+-O_w RDF as a function of temperature in 0.1 molal aqueous NaCl solution and inside the grafted PE layer with $\sigma_g = 0.1/\sigma^2$.

Translational mobility of counterions

From Fig. 10, we observe that the counterion mobility (as quantified by their mean squared displacement or MSD) increases with an increase in temperature for a given grafting density. This behavior is expected due to the enhanced thermal fluctuations at higher temperatures. However, the increase in counterion MSD is not very prominent (see the scale on the y-axis of Fig. 10). The counterions show sub-diffusive behavior even at elevated temperatures. This can be attributed to an increase in the number of $O_{Carboxylate}$ atoms solvating the counterions with increase in temperature [see Fig. 8(a) and Fig. S7(a)]. In other words, the counterions are condensed on a larger number of $O_{Carboxylate}$ atoms (on an average) at higher temperatures. As a result, they are unable to escape the electrostatic binding with the PE functional groups despite their enhanced thermal energy.

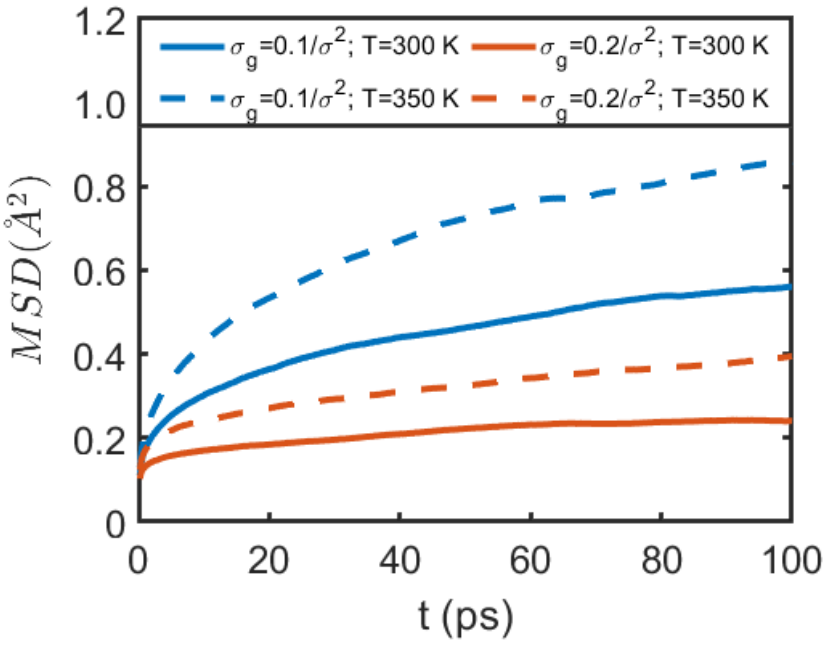

Figure 10: Mean squared displacement (MSD) of counterions inside the PE brush layer for various combinations of temperatures and grafting densities.

Methods

Our simulation domain consisted of 36 fully ionized PAA chains H[-(CH_2-$CH(COO^-)$-]$_n$$CH_3$ grafted in a 6 x 6 square array. One terminal carbon atom of each chain was fixed to the grafting plane (z=0) to form the "brush"-like configuration. Each PAA chain consisted of 49 backbone carbon atoms. Two different grafting densities, $\sigma_g = 0.1/\sigma^2,\ 0.2/\sigma^2$ [$\sigma = 3.5$ Å is the Lennard Jones (LJ) distance parameter associated with the backbone carbon atoms of the PAA chains] were probed by varying the distance between the grafted ends of adjacent chains (ℓ), with $\ell = 1/\sqrt{\sigma_g}$. Our grafting densities of $0.1/\sigma^2$ (corresponding to 0.82 chains/nm^2) and $0.2/\sigma^2$ (corresponding to 1.63 chains/nm^2) are well within the range of values reported by prior experiments on PAA brushes (0.12 - 2.5 chains/nm^2).[65] For each value of grafting density, simulations were carried out for three different system temperatures, T=300 K, 325 K, and 350 K. The charges on the PE chains were neutralized by adding 864 Na^+ counterions to the system. SPC/E water molecules were added to the system to act as a "good" solvent for the PAA chains.[66] Enough water molecules were added to ensure that the height of the simulation domain is at least 1.5 Nσ. No external salt (ion pairs) was added to the system. Two discrete walls made of a single layer of particles arranged in an FCC lattice (with a lattice constant of 3.612 Å) were placed at the top and bottom of the simulation domain to prevent the mobile species from leaving the system. These walls were fixed in the x and y directions but allowed to translate freely as a rigid body along the z direction.

The PAA chains were modelled using the OPLS-AA force field.[67] Both bonded (bonds, angles, dihedrals, and impropers) and non-bonded (partial charges and LJ parameters) interaction parameters for the various atom types of the PAA chains were taken from the OPLS database and have been provided in our prior publication (see the Supporting Information for Ref. 43). The LJ

parameters for the Na^+ counterions were obtained from the work of Joung *et al*.[68] Geometric mixing rules were used for modeling the LJ interactions between dissimilar atom types. The only exception to this rule were the LJ interactions between the oxygen atoms of water molecules and the Na^+ counterions, which used Lorentz-Berthelot mixing rules in accordance with Joung *et al* (Ref. 68). All LJ interactions were modelled using a shifted, truncated 12-6 Lennard Jones potential with a 13 Å cut off. The long-range coulombic interactions were calculated using a particle-particle particle-mesh (PPPM) solver.[69] Periodic boundary conditions were used in the x and y directions, while a fixed boundary condition was used in the z direction or the direction perpendicular to the grafting plane. The SHAKE algorithm[70] was used to ensure rigid bonds and angles associated with the SPC/E water molecules.

The initial configuration of the system consisted of an array of fully stretched PAA chains along with a line of counterions placed next to them. The SPC/E water molecules were distributed throughout the simulation domain. The system was first simulated in an NP_zT ensemble (the subscript z represents that only the height of the simulation domain was allowed to change to maintain a constant pressure) to obtain the correct height of the simulation domain. The temperature and pressure of the system were maintained at 300 K and 1 atm respectively by using a Nosé-Hoover thermostat and barostat,[71-72] with time constant of 0.1 ps (for temperature) and 1 ps (for pressure). Then, the system was equilibrated in the canonical (NVT) ensemble. Two separate Langevin thermostats[73] (with time constants of 0.1 ps) were used to maintain the temperature of the PAA chains and the mobile species (water molecules and counterions) at 300 K. The brush height of the PAA chains was constantly monitored to check for proper equilibration (see Fig. S1 in the SI for the autocorrelation function corresponding to the average end-to-end brush height; see Table S1 for the average end-to-end brush height, equilibration time, and

production run time corresponding to various temperatures and PE brush grafting densities). The equilibration was followed by a production run of 2 ns. This served as the starting configuration for the simulations at higher temperatures. i.e., 325 K and 350 K. Starting from the fully equilibrated system configuration at 300 K, the temperature was ramped up to the desired value (in a step-like jump) and the system was allowed to equilibrate under the NVT ensemble. Thermostating was done in a similar fashion as before (i.e., for the case of 300 K). Again, proper equilibration was ensured by monitoring the average end-point brush height, followed by a production run of 4-5 ns.

All simulations were run on the MD simulation package LAMMPS (Large-scale Atomic/Molecular Massively Parallel Simulator).[74] The particle trajectories were calculated using the velocity Verlet algorithm with a time step of 2 fs. All the atomic coordinates were dumped every 1000 fs. In addition, the coordinates of the atom types associated with the PAA chains and counterions were dumped separately every 200 fs. The particles were visualized using the open-source software OVITO.[75]

Conclusions

We have utilized all-atom MD simulations to investigate the influence of temperature on the "microstructure" of strongly water-swollen PE brushes, and how these changes at the atomistic level affect the properties of the brushes at much larger length scales (e.g., variation in the equilibrium brush height). Our results indicate a reduction in the average end-point brush height with increase in temperature, which is in excellent agreement with prior theoretical[45] and experimental[48] studies. The reduction in brush height is a consequence of the decrease in solvent quality at elevated temperatures, brought about by a decrease in the free energy favorability of the formation of the water-water and water-PE HBs. The reduction in brush height is accompanied by an expulsion of water molecules from the grafted PE layer to the bulk. This expulsion of water increases the PE volume fraction inside the brushes, which in conjunction with the reduced HB strength leads to a decrease in the fraction of water-water and water-PE HBs (within the grafted PE layer) with temperature. In addition, the kinetics of water-water and water-PE HB decay also becomes faster at higher temperatures, as quantified by the HB residence time. The severing of water-water HBs shifts the distribution of the orientational tetrahedral order parameter towards lower values (indicating larger deviations from a tetrahedral arrangement), although the extent of this shift is much lesser inside the brushes as compared to bulk. Our results establish that the self-diffusion coefficient (calculated via the mean squared displacement) of water inside the brushes follows the Arrhenius equation, and that the corresponding activation energy increases monotonically with increase in the degree of PE brush-induced nanoconfinement. We also observe significant changes in the properties of the brush-supported counterions with temperature. There is an enhanced replacement of the solvation water of the counterions by $O_{Carboxylate}$ atoms (inside the PE brushes) at elevated temperatures since the water molecules lose significant entropy while

solvating (or being 'bound' to) the counterions. This enhanced replacement of solvation water is also witnessed in the form of a reduced first peak height of the Na^+-O_w RDF at higher temperatures. The decrease in mass density of water (within the brushes) at higher temperatures manifests as an increased propensity of the PE-brush-water-counterion system to exhibit "water-in-salt"-like behavior, where the water supersedes the 'salt' (in this case the PE repeating unit-counterion complex) by both mass and volume. Finally, the counterion mobility inside the brushes increases with temperature, albeit not by much as the counterions are unable to escape the coulombic interactions with the negatively charged PE functional groups.

In conclusion, our study bridges the gap between atomistic (a few angstroms) and molecular (multiple nanometers) length scales by explaining how a parameter as fundamental as temperature is able to affect the "microstructure" of the brushes (e.g., properties of water-water and water-PE HBs), and how these changes at the atomistic length scales can help us understand variations in experimentally measurable quantities (e.g., the PE brush height). In the present study, we only consider fully ionized PAA brushes without the presence of an added salt, which means that our results are applicable only under specific conditions. The effect of degree of ionization of the PE chains (due to changes in pH of the system) as well as the concentration of an added salt on the temperature response of the brushes are important problems to study. However, given the complete lack of all-atom MD studies investigating the temperature response of water-swollen PE brushes (to the best of our knowledge), the current manuscript will help kickstart a discussion on the topic. In the future, we plan to further expand our knowledge by investigating the effects of the degree of ionization of the PE chains, concentration of added salt, nature of added salt (by varying the size and valence of the cations of the salt), etc. on the temperature response of water-swollen PE brushes.

Acknowledgement

This work has been supported by the Department of Energy Office of Science grant DE-SC0017741. We would like to express our gratitude to Dr. Peter W. Chung at the University of Maryland, College Park for providing his personal computational resources for carrying out a few of the simulations. Analysis of the results and some simulations were conducted on the high-performance cluster Deepthought2.

Supporting Information

Autocorrelation function for average end-to-end brush height; transverse distribution of the fraction of water-water HBs; probability distribution of the number of water-water HBs formed by water molecules; mean squared displacement of PE brush-trapped water molecules; percentage of 'bound' water molecules; results for higher grafting density.

References

1. Zhulina, E. B.; Rubinstein, M. Lubrication by Polyelectrolyte Brushes. *Macromolecules* **2014**, *47*, 5825−5838.

2. Chen, G.; Sachar, H. S.; Das, S. Efficient Electrochemomechanical Energy Conversion in Nanochannels Grafted with End-Charged Polyelectrolyte Brushes at Medium and High Salt Concentration. *Soft Matter* **2018**, *14*, 5246−5255.

3. Sachar, H. S.; Sivasankar, V. S.; Das, S. Electrokinetic Energy Conversion in Nanochannels Grafted with pH-responsive Polyelectrolyte Brushes Modelled using Augmented Strong Stretching Theory. *Soft Matter* **2019**, *15*, 5973–5986.

4. Ali, M.; Yameen, B.; Cervera, J.; Ramírez, P.; Neumann, R.; Ensinger, W.; Knoll, W.; Azzaroni, O. Layer-by-layer Assembly of Polyelectrolytes into Ionic Current Rectifying Solid-state Nanopores: Insights from Theory and Experiment. *J. Am. Chem. Soc*. **2010**, *132*, 8338−8348.

5. Yameen, B.; Ali, M.; Neumann, R.; Ensinger, W.; Knoll, W.; Azzaroni, O. Single Conical Nanopores Displaying pH-Tunable Rectifying Characteristics. Manipulating Ionic Transport with Zwitterionic Polymer Brushes. *J. Am. Chem. Soc*. **2009**, *131*, 2070.

6. Perez Sirkin, Y. A.; Szleifer, I.; Tagliazucchi, M. Voltage-Triggered Structural Switching of Polyelectrolyte-Modified Nanochannels. *Macromolecules*, **2020**, *53*, 2616−2626.

7. Yang, Q.; Li, L.; Zhao, F.; Han, H.; Wang, W.; Tian, Y.; Wang, Y.; Ye, Z.; Guo, X. Hollow Silica-polyelectrolyte Composite Nanoparticles for Controlled Drug Delivery. *J. Mater. Sci*. **2019**, *54*, 2552−2565.

8. Saraswathy, M.; Gong, S. Recent Developments in the CoDelivery of siRNA and Small Molecule Anticancer Drugs for Cancer Treatment. *Mater. Today* **2014**, *17*, 298−306.

9. ShamsiJazeyi, H.; Miller, C. A.; Wong, M. S.; Tour, J. M.; Verduzco, R. Polymer-coated Nanoparticles for Enhanced Oil Recovery. *J. Appl. Polym. Sci*. **2014**, *131*, 40576.

10. Motornov, M.; Sheparovych, R.; Lupitskyy, R.; MacWilliams, E.; Hoy, O.; Luzinov, I.; Minko, S. Stimuli-Responsive Colloidal Systems from Mixed Brush-Coated Nanoparticles. *Adv. Funct. Mater.* **2007**, *17*, 2307.

11. Pincus, P. Colloid Stabilization with Grafted Polyelectrolytes. *Macromolecules* **1991**, *24*, 2912–2919.

12. Ross, R. S.; Pincus, P. The Polyelectrolyte Brush: Poor Solvent. *Macromolecules* **1992**, *25*, 2177–2183.

13. Miklavic, S. J.; Marcelja, S. Interaction of Surfaces Carrying Grafted Polyelectrolytes. *J. Phys. Chem.* **1988**, *92*, 6718–6722.

14. Misra, S.; Varanasi, S.; Varanasi, P. P. A Polyelectrolyte Brush Theory. *Macromolecules* **1989**, *22*, 4173–4179.

15. Borisov, O. V.; Birshtein, T. M.; Zhulina, E. B. Collapse of Grafted Polyelectrolyte Layer. *J. Phys. II* **1991**, *1*, 521–526.

16. Zhulina, E. B.; Rubinstein, M.; Ionic Strength Dependence of Polyelectrolyte Brush Thickness. *Soft Matter* **2012**, *8*, 9376–9383.

17. Zhulina, E. B.; Borisov, O. V. Structure and Interaction of Weakly Charged Polyelectrolyte Brushes: Self-Consistent Field Theory. *J. Chem. Phys.* **1997**, *107*, 5952–5967.

18. Zhulina, E. B.; Borisov, O. V. Poisson–Boltzmann Theory of pH-Sensitive (Annealing) Polyelectrolyte Brush. *Langmuir* **2011**, *27*, 10615–10633.

19. Mei, Y.; Lauterbach, K.; Hoffmann, M.; Borisov, O. V.; Ballauff, M.; Jusufi, A. Collapse of Spherical Polyelectrolyte Brushes in the Presence of Multivalent Counterions. *Phys. Rev. Lett.* **2006**, *97*, 158301.

20. Sachar, H. S.; Sivasankar, V. S.; Das, S. Revisiting the Strong Stretching Theory for pH-Responsive Polyelectrolyte Brushes: Effects of Consideration of Excluded Volume Interactions and an Expanded form of the Mass Action Law. *Soft Matter* **2019**, *15*, 559–574.

21. Csajka, F. S.; Seidel, C. Strongly Charged Polyelectrolyte Brushes: A Molecular Dynamics Study. *Macromolecules* **2000**, *33*, 2728–2739.

22. He, G. L.; Merlitz, H.; Sommer, J. U. Molecular Dynamics Simulations of Polyelectrolyte Brushes under Poor Solvent Conditions: Origins of Bundle Formation. *J. Chem. Phys.* **2014**, *140*, 104911.

23. Sandberg, D. J.; Carrillo, J. M. Y.; Dobrynin, A. V. Molecular Dynamics Simulations of Polyelectrolyte Brushes: From Single Chains to Bundles of Chains. *Langmuir* **2007**, *23*, 12716–12728.

24. Desai, P. R.; Sinha, S.; Das, S. Polyelectrolyte Brush Bilayers in Weak Interpenetration Regime: Scaling Theory and Molecular Dynamics Simulations. *Phys. Rev. E* **2018**, *97*, 032503.

25. Mei, Y.; Hoffmann, M.; Ballauff, M.; Jusufi, A. Spherical Polyelectrolyte Brushes in the Presence of Multivalent Counterions: The Effect of Fluctuations and Correlations as Determined by Molecular Dynamics Simulations. *Phys. Rev. E* **2008**, *77*, 031805.

26. Carrillo, J. M. Y.; Dobrynin, A. V. Morphologies of Planar Polyelectrolyte Brushes in a Poor Solvent: Molecular Dynamics Simulations and Scaling Analysis. *Langmuir* **2009**, *25*, 13158–13168.

27. Hehmeyer, O. J.; Stevens, M. J. Molecular Dynamics Simulations of Grafted Polyelectrolytes on Two Apposing Walls. *J. Chem. Phys.* **2005**, *122*, 134909.

28. Jackson, N. E.; Brettmann, B. K.; Vishwanath, V.; Tirrell, M.; de Pablo, J. J. Comparing Solvophobic and Multivalent Induced Collapse in Polyelectrolyte Brushes. *ACS Macro Lett.* **2017**, *6*, 155–160.

29. Merlitz, H.; Li, C.; Wu, C.; Sommer, J. U. Polyelectrolyte Brushes in External Fields: Molecular Dynamics Simulations and Mean-Field Theory. *Soft Matter* **2015**, *11*, 5688–5696.

30. Kumar, N. A.; Seidel, C. Polyelectrolyte Brushes with Added Salt. *Macromolecules* **2005**, *38*, 9341–9350.

31. Wittemann, A.; Drechsler, M.; Talmon, Y.; Ballauff, M. High Elongation of Polyelectrolyte Chains in the Osmotic Limit of Spherical Polyelectrolyte Brushes: A Study by Cryogenic Transmission Electron Microscopy. *J. Am. Chem. Soc.* **2005**, *127*, 9688–9689.

32. Biesalski, M.; Johannsmann, D.; Rühe, J. Electrolyte-Induced Collapse of a Polyelectrolyte Brush. *J. Chem. Phys.* **2004**, *120*, 8807–8814.

33. Balastre, M.; Li, F.; Schorr, P.; Yang, J.; Mays, J. W.; Tirrell, M. V. A Study of Polyelectrolyte Brushes Formed from Adsorption of Amphiphilic Diblock Copolymers Using the Surface Forces Apparatus. *Macromolecules* **2002**, *35*, 9480–9486.

34. Yu, J.; Jackson, N. E.; Xu, X.; Morgenstern, Y.; Kaufman, Y.; Ruths, M.; de Pablo, J. J.; Tirrell, M. Multivalent Counterions Diminish the Lubricity of Polyelectrolyte Brushes. *Science* **2018**, *360*, 1434–1438.

35. Yu, J.; Jackson, N. E.; Xu, X.; Brettmann, B. K.; Ruths, M.; de Pablo, J. J.; Tirrell, M. Multivalent Ions Induce Lateral Structural Inhomogeneities in Polyelectrolyte Brushes. *Sci. Adv.* **2017**, *3*, eaao1497.

36. Yu, J.; Mao, J.; Yuan, G.; Satija, S.; Chen, W.; Tirrell, M. The Effect of Multivalent Counterions to the Structure of Highly Dense Polystyrene Sulfonate Brushes. *Polymer* **2016**, *98*, 448–453.

37. Yu, J.; Mao, J.; Yuan, G.; Satija, S.; Jiang, Z.; Chen, W.; Tirrell, M. Structure of Polyelectrolyte Brushes in the Presence of Multivalent Counterions. *Macromolecules* **2016**, *49*, 5609–5617.

38. Mahalik, J. P.; Yang, Y.; Deodhar, C.; Ankner, J. F.; Lokitz, B. S.; Kilbey, S. M.; Sumpter, B. G.; Kumar, R. Monomer Volume Fraction Profiles in pH Responsive Planar Polyelectrolyte Brushes. *J. Polym. Sci., Part B: Polym. Phys.* **2016**, *54*, 956–964.

39. Farina, R.; Laugel, N.; Pincus, P.; Tirrell, M. Brushes of Strong Polyelectrolytes in Mixed Mono-and Tri-Valent Ionic Media at Fixed Total Ionic Strengths. *Soft Matter* **2013**, *9*, 10458–10472.

40. Schneider, C.; Jusufi, A.; Farina, R.; Pincus, P.; Tirrell, M.; Ballauff, M. Stability Behavior of Anionic Spherical Polyelectrolyte Brushes in the Presence of La (III) Counterions. *Phys. Rev. E* **2010**, *82*, 011401.

41. Sachar, H. S.; Pial, T. H.; Desai, P. R.; Etha, S. A.; Wang, Y.; Chung, P. W.; Das, S. Densely Grafted Polyelectrolyte Brushes Trigger "Water-in-Salt"-like Scenarios and Ultraconfinement Effect. *Matter* **2020**, *2*, 1509–1521.

42. Sachar, H. S.; Pial, T. H.; Chava, B. S.; Das, S. All-atom Molecular Dynamics Simulations of Weak Polyionic Brushes: Influence of Charge Density on the Properties of Polyelectrolyte Chains, Brush-supported Counterions, and Water Molecules. *Soft Matter* **2020**, *16*, 7808−7822.

43. Sachar, H. S.; Chava, B. S.; Pial, T. H.; Das, S. Hydrogen Bonding and Its Effect on the Orientational Dynamics of Water Molecules inside Polyelectrolyte Brush-Induced Soft and Active Nanoconfinement. *Macromolecules* **2021**, *54*, 2011−2021.

44. Dormidontova, E. E. Role of Competitive PEO−Water and Water−Water Hydrogen Bonding in Aqueous Solution PEO Behavior. *Macromolecules* **2002**, *35*, 987−1001.

45. Ren, C.-l.; Nap, R. J.; Szleifer, I. The Role of Hydrogen Bonding in Tethered Polymer Layers. *J. Phys. Chem. B* **2008**, *112*, 16238−16248.

46. Dahal, U. R.; Wang, Z.; Dormidontova, E. E. Hydration and Mobility of Poly(ethylene oxide) Brushes. *Macromolecules* **2017**, *50*, 6722−6732.

47. Dahal, U.; Wang, Z.; Dormidontova, E. E. Hydration of Spherical PEO-grafted Gold Nanoparticles: Curvature and Grafting Density Effect. *Macromolecules* **2018**, *51*, 5950−5961.

48. Zhuang, P.; Dirani, A.; Glinel, K.; Jonas, A. M. Temperature Dependence of the Surface and Volume Hydrophilicity of Hydrophilic Polymer Brushes. *Langmuir* **2016**, *32*, 3433−3444.

49. Suo, L.; Borodin, O.; Gao, T.; Olguin, M.; Ho, J.; Fan, X.; Luo, C.; Wang, C.; Xu, K. "Water-in-salt" Electrolyte Enables High-voltage Aqueous Lithium-ion Chemistries. *Science* **2015**, *350*, 938−943.

50. Han, S. Dynamic Features of Water Molecules in Superconcentrated Aqueous Electrolytes. *Sci. Rep*. **2018**, *8*, 9347.

51. Flory, P. J. Principles of Polymer Chemistry. *Cornell University Press* **1953**.

52. Baulin, V. A.; Zhulina, E. B.; Halperin, A. Self-Consistent Field Theory of Brushes of Neutral Water-Soluble Polymers. *J. Chem. Phys.* **2003**, *119*, 10977−10988.

53. Baulin, V. A.; Halperin, A. Signatures of a Concentration-Dependent Flory χ Parameter: Swelling and Collapse of Coils and Brushes. *Macromol. Theory Simul.* **2003**, *12*, 549−559.

54. Morochnik, S.; Nap, R. J.; Ameer, G. A.; Szleifer, I. Structural Behavior of Competitive Temperature and pH-responsive Tethered Polymer Layers. *Soft Matter* **2017**, *13*, 6322−6331.

55. Alexander, S. Adsorption of Chain Molecules with a Polar Head a Scaling Description. *J. Phys.* **1977**, *38*, 983−987.

56. De Gennes, P. G. Scaling Theory of Polymer Adsorption. *J. Phys.* **1976**, *37*, 1445−1452.

57. Ritsema van Eck, G. C.; Veldscholte, L. B.; Nijkamp, J. H.; de Beer, S. Sorption Characteristics of Polymer Brushes in Equilibrium with Solvent Vapors. *Macromolecules* **2020**, *53*, 8428−8437.

58. Smook, L. A.; Ritsema van Eck, G. C.; de Beer, S. Friends, Foes, and Favorites: Relative Interactions Determine How Polymer Brushes Absorb Vapors of Binary Solvents. *Macromolecules* **2020**, 53, 10898−10906.

59. Duboué-Dijon, E.; Laage, D. Characterization of the Local Structure in Liquid Water by Various Order Parameters. *J. Phys. Chem. B* **2015**, *119*, 8406−8418.

60. Nayar, D.; Agarwal, M.; Chakravarty, C. Comparison of Tetrahedral Order, Liquid State Anomalies, and Hydration Behavior of mTIP3P and TIP4P Water Models. *J. Chem. Theory Comput.* **2011**, *7*, 3354−3367.

61. Jabes, B. S.; Nayar, D.; Dhabal, D.; Molinero, V.; Chakravarty, C. Water and Other Tetrahedral Liquids: Order, Anomalies and Solvation. *J. Phys. Condens. Matter* **2012**, *24*, 284116.

62. Lee, S. L.; Debenedetti, P. G.; Errington, J. R. A Computational Study of Hydration, Solution Structure, and Dynamics in Dilute Carbohydrate Solutions. *J. Chem. Phys.* **2005**, *122*, 204511.

63. He, X.; Zhu, Y.; Epstein, A.; Mo, Y. Statistical Variances of Diffusional Properties from Ab Initio Molecular Dynamics Simulations. *Npj Comput. Mater.* **2018**, *4*, 1−9.

64. Lee, S. H. Temperature Dependence on Structure and Self-diffusion of Water: A Molecular Dynamics Simulation Study using SPC/E Model. *B. Korean Chem. Soc.* **2013**, *34*, 3800−3804.

65. Hollingsworth, N. R.; Wilkanowicz, S. I.; Larson, R. G. Salt-and pH-induced Swelling of a poly(acrylic acid) Brush via Quartz Crystal Microbalance w/dissipation (QCM-D). *Soft Matter* **2019**, *15*, 7838−7851.

66. Berendsen, H. J. C.; Grigera, J. R.; Straatsma, T. P. The Missing Term in Effective Pair Potentials. *J. Phys. Chem*. **1987**, *91*, 6269−6271.

67. Jorgensen, W. L.; Maxwell, D. S.; TiradoRives, J. Development and Testing of the OPLS All-Atom Force Field on Conformational Energetics and Properties of Organic Liquids. *J. Am. Chem. Soc.* **1996**, *118*, 11225−11236.

68. Joung, I. S.; Cheatham, T. E. Determination of Alkali and Halide Monovalent Ion Parameters for Use in Explicitly Solvated Biomolecular Simulations. *J. Phys. Chem. B* **2008**, *112*, 9020−9041.

69. Hockney, R. W.; Eastwood, J. W.; Computer Simulations Using Particles. *mcgraw-hill. New York.* **1981**.

70. Ryckaert, J.-P.; Ciccotti, G.; Berendsen, H. J. Numerical Integration of the Cartesian Equations of Motion of a System with Constraints: Molecular Dynamics of n-alkanes. *J. Comput. Phys.* **1977**, *23*, 327−341.

71. Hoover, W. G. Canonical Dynamics: Equilibrium Phase-Space Distributions. *Phys. Rev. A* **1985**, *31*, 1695−1697.

72. Nosé, S. A Unified Formulation of the Constant Temperature Molecular Dynamics Methods. *J. Chem. Phys.* **1984**, *81*, 511–519.

73. Schneider, T.; Stoll, E. Molecular-dynamics Study of a Three Dimensional One-component Model for Distortive Phase Transitions. *Phys. Rev. B* **1978**, *17*, 1302−1322.

74. Plimpton, S. J. Fast Parallel Algorithms for Short-Range Molecular Dynamics. *J. Comput. Phys*. **1995**, *117*, 1−19.

75. Stukowski, A. Visualization and Analysis of Atomistic Simulation Data with OVITO–the Open Visualization Tool. *Model. Simul. Mater. Sci. Eng*. **2010**, *18*, 015012.